Journal of Applied Horticulture, 28(1): 3-10, 2026
https://doi.org/10.37855/jah.2026.v28i01.1
Journal of Applied Horticulture
ISSN: 0972-1045

Computer vision-based non-invasive biomass estimation and water stress monitoring in tomato plants

P. Hemamalini[1,2], M.K. Chandraprakash[1], K. Suneetha[2] and R.H. Laxman[1]*

*[1]ICAR-Indian Institute of Horticultural Research, Bengaluru, India. [2]Jain (Deemed-to-be) University, Bengaluru, India. *E-mail: laxmaniihr@gmail.com*

Abstract

Precision horticulture demands intelligent monitoring systems for automated crop management. While traditional biomass estimation relies on destructive sampling, modern ICT-driven approaches offer transformative solutions. This study presents an AI-powered methodology integrating YOLOv11 for autonomous biomass estimation and stress monitoring in tomato crops. High-resolution RGB imagery was captured across multiple phenological stages under two irrigation regimes. YOLOv11's computer vision capabilities enabled automated canopy detection, segmentation, and digital biomass quantification, eliminating destructive sampling. Novel AI-driven metrics were introduced: convex hull area for stress-induced canopy alterations and compactness (digital biomass to convex hull ratio) for automated canopy assessment. This integrated approach achieved robust accuracy in stress detection and biomass estimation (R^2 =0.821), enabling real-time monitoring for precision horticulture. The model demonstrated exceptional performance with segmentation precision of 0.950, recall of 0.979, and mean average precision of 0.975 at IoU 0.5, with mAP50-95 of 0.826. The rapid inference time of 2.3ms per image enables high-throughput phenotyping and decision support for site-specific management. YOLOv11-derived digital biomass correlated strongly with fresh biomass (R^2 = 0.821). Image-derived features effectively differentiated control and stress conditions. Genotype analysis revealed variation in biomass accumulation: Arka Abhed and Arka Rakshak performed better under optimal irrigation, while Arka Vikas showed greater stress resilience. These results validate YOLOv11 as a scalable solution for intelligent crop monitoring and precision input application in next-generation digital horticulture.

Key words: Precision agriculture, image segmentation, deep learning, biomass, stress, digital phenotyping

Introduction

Tomato plants are among the most widely cultivated horticultural crops, serving as a vital source of nutrition and economic value worldwide (Ritchie *et al.,* 2023). Monitoring their growth and stress responses is critical for optimizing yield and resource efficiency. Mahdy *et al*. (2024) reported significant alterations in growth and physiological attributes of tomato under salt stress, highlighting the importance of accurately assessing growth responses under stress conditions. Traditional methods such as destructive sampling for estimating plant biomass and detecting stress are becoming increasingly impractical (Wu *et al.,* 2024). These methods involve harvesting and weighing plants, which is time-consuming and disrupts plant growth, making them less feasible in the context of modern agricultural challenges (Decker *et al.,* 2018).

Biomass estimation is a cornerstone of plant growth analysis, providing insights into crop development, yield potential, and resource utilization efficiency (Hagn *et al.,* 2024). By quantifying biomass through various growth stages, researchers can better understand the influence of environmental conditions on crop development (Laxman *et al.,* 2018). In addition to growth analysis, biomass estimation plays a pivotal role in stress detection. Stress conditions, such as water deficit and extreme temperatures, significantly affect the physiological and morphological traits of tomato plants. Rahman *et al*. (2025) observed improved salinity tolerance in tomato through hormonal regulation, reinforcing the link between stress physiology and biomass production. These changes often manifest as reductions in biomass, alterations in canopy structure, and decreased growth rates (Rocha Júnior *et al.,* 2023). Estimating biomass through image-derived parameters has become highly efficient and accessible with advancements in high-resolution RGB imaging. By leveraging RGB images, researchers can non-invasively extract key metrics, such as digital biomass, canopy area, and plant structural attributes (Laxman *et al.,* 2022). These images capture fine details of plant morphology, enabling precise biomass quantification without destructive sampling. Such approaches are particularly relevant in the context of studies reporting improved tomato growth under optimized cultivation and management practices (James and Umesh, 2025)

Advanced image analysis techniques, combined with machine learning models, facilitate the segmentation and measurement of plant canopies directly from RGB images (Johansen *et al.,* 2020). Metrics such as pixel area, convex hull dimensions, and canopy density can be precisely quantified, offering valuable insights into plant growth dynamics and responses to environmental stressors (Tripodi *et al.,* 2024). Among these advancements, the adoption of computer vision and machine learning technologies has revolutionized the way plant attributes are monitored and quantified (Li *et al.,* 2022). Furthermore, these approaches offer a non-destructive, rapid, and scalable solution for large-scale phenotyping (Smith *et al.,* 2021), resource management, and stress monitoring, aligning perfectly with the goals of precision agriculture.

Among deep learning models, YOLO (You Only Look Once) has emerged as a frontrunner for its real-time detection and segmentation capabilities, making it particularly suitable for agricultural applications (Redmon *et al.,* 2016). The YOLO models, renowned for their speed and scalability (Paul *et al.*, 2024), integrate detection and segmentation tasks into a unified framework (Desai and Kore, 2025). This efficiency is especially beneficial for large-scale phenotyping and stress monitoring, where high throughput and real-time processing are critical (Jain *et al.,* 2024. The recently released YOLO11 represents a significant advancement in the evolution of YOLO models, incorporating several enhancements that improve both accuracy and efficiency. The advancements introduced by YOLO11 (Khanam and Hussain, 2024), significantly enhance its capability for precise segmentation and object detection in agricultural applications. This efficiency makes it particularly suitable for large-scale phenotyping and real-time biomass estimation in agricultural applications.

The primary objective of this study is to develop a robust, non-invasive, and scalable approach for biomass estimation and stress detection in tomato plants using YOLO11. The study aimed to achieve the following specific goals: Accurately segment plant canopy and compute digital biomass metrics across different growth stages and irrigation regimes, providing real-time, non-destructive measurements for continuous monitoring and decision-making. Also to evaluate the statistical sensitivity of Convex Hull Area and Compactness as non-invasive stress indicators, specifically determining their ability to significantly differentiate between well-watered and water-stressed plants.

By connecting advanced imaging technologies with plant science, this study aims to bridge the gap between technological innovation and practical agricultural applications, paving the way for sustainable and data-driven crop management.

Materials and methods

Experimental setup: The study was conducted under open-field conditions during the cropping season from July to September 2023 at the ICAR-Indian Institute of Horticultural Research, Bengaluru, India (13.14°N, 77.58°E). Four tomato genotypes—Arka Rakshak, Arka Abhed, Arka Vikas, and Arka Meghali—were evaluated under two distinct irrigation regimes: 100% Field Capacity (FC) and 50% FC, representing control and water-stress conditions, respectively. High-resolution RGB images were captured at two critical growth stages, flowering and fruiting, to assess morphological and physiological responses to two irrigation levels (100% FC and 50% FC). For validation purposes, fresh plant biomass was measured using destructive sampling on a subset of 100 representative samples. This provided ground truth data to assess the accuracy of the digital biomass estimates derived from the segmented canopy images.

Image Acquisition and Annotation: High-resolution RGB images were captured using a Nikon DSLR camera with a 12-megapixel resolution. Images were acquired with the camera configured to an aperture of f/8.0 to ensure adequate depth of field for the entire canopy, and a sensitivity of ISO 200 to minimize sensor noise. The camera was mounted on a field imaging system to ensure consistent image framing and optimal angles during data collection. Images were predominantly captured during morning hours to ensure uniform lighting conditions. A total of 940 images were collected across four genotypes, two growth stages (flowering and fruiting), and two irrigation regimes (100% FC and 50% FC). The collected images were annotated for segmentation using the Roboflow platform, with the target class labeled "Canopy" to ensure precise identification and segmentation of plant structures. Precise labels corresponding to canopy boundaries were generated to train the YOLOv11 segmentation model, enabling accurate detection and quantification of plant biomass and associated parameters.

YOLO11 Model Architecture: The YOLOv11 architecture represents a significant advancement in object detection and segmentation, designed to optimize both speed and accuracy. Building on the innovations of earlier YOLO versions, it introduces key components such as the C3K2 block, SPFF module (Spatial Pyramid Pooling Fast), and C2PSA block (Cross Stage Partial with Spatial Attention) to enhance feature extraction and detection capabilities. The backbone employs convolutional blocks, bottlenecks, and the advanced C3K2 structure, which improves computational efficiency and feature representation by leveraging smaller kernel convolutions and a refined CSP-inspired design. In the neck, the SPFF module aggregates multi-scale contextual information via efficient max pooling, ensuring robust object detection across varying scales, including smaller and partially occluded objects. The C2PSA block in the neck incorporates spatial attention mechanisms to refine feature maps, enhancing the model's ability to focus on regions of interest while maintaining computational efficiency. The detection head utilizes multi-scale predictions from three feature levels (P3, P4, and P5), allowing the model to detect objects of various sizes with high precision. These advancements make YOLOv11 particularly well-suited for applications requiring real-time segmentation and detection, including agricultural tasks such as plant canopy segmentation and biomass estimation.

Model Training: The YOLOv11 model was trained and validated to accurately segment tomato plant canopies and extract key parameters for biomass estimation and stress detection. The process involved preparing annotated datasets, implementing appropriate training configurations, and evaluating model performance to ensure reliability and generalizability. The dataset is split into training, validation and test with 840, 80 and 40 images respectively. The training parameters are given in the Table below

Table 1. Training parameters for YOLO11 model

Parameter	Value	Description
Learning rate	0.001	Initial rate for adjusting weights during training
Batch size	16	Number of images processed in each training iteration
No. of epochs	100	Total number of passes through the training dataset
Image size	640 x 640	Resized dimensions of input images for YOLOv11

Digital biomass parameter extraction: Post-segmentation, several morphological features were extracted from the predicted masks to characterize plant biomass and structural properties. The primary parameters included plant area (total number of pixels within the segmented canopy region, converted to

square centimeters using calibration factors), convex hull area (area of the smallest convex polygon enclosing the plant), and compactness (ratio of plant area to convex hull area, indicating canopy density and structural complexity). Additional features, including perimeter, major axis length, minor axis length, and eccentricity, were also computed to provide comprehensive morphological characterization. These parameters were correlated with manually measured fresh weight biomass to validate their predictive capability.

Statistical analysis: Linear regression was conducted to correlate digital biomass with traditional biomass measurements, achieving an $R^2 = 0.821$ ($P< 0.001$; n = 100). Linear regression was performed using pooled observations across genotypes, growth stages, and irrigation treatments to validate the relationship between image-derived digital biomass and fresh weight. Regression assumptions were evaluated using residual normality tests, heteroscedasticity diagnostics, and influence statistics. Three-way ANOVA was performed with genotype (4 levels), irrigation regime (2 levels: 100% FC and 50% FC), and growth stage (2 levels: flowering and fruiting) as fixed factors, with three biological replications per treatment combination. Duncan's Multiple Range Test (DMRT) was applied as post-hoc test for mean separation at $P< 0.05$. Statistical analyses were conducted using Python.

Hardware and software: The YOLOv11 model and image processing tasks were implemented in Google Colab, running on an NVIDIA A100 GPU, providing the computational power required for training and validation. The platform allowed for efficient execution of deep learning workflows, leveraging its high-performance hardware and seamless integration with Python-based machine learning libraries. The software environment was set up with Python (version 3.8) as the primary programming language. Key libraries and frameworks included PyTorch for deep learning model implementation, OpenCV for image preprocessing, and Matplotlib for visualizing results. Annotation and dataset preparation were facilitated using the Roboflow platform, while training configurations were managed via custom scripts executed on Colab.

Results

The model demonstrated smooth convergence, with both training and validation losses decreasing consistently over the epochs (Fig. 1). The validation loss stabilized after 70 epochs, indicating that the model had achieved optimal learning without overfitting.

The convergence of loss values highlights the effectiveness of the YOLOv11 architecture in learning segmentation patterns from annotated images. The minimal gap between training and validation losses underscores the model's generalizability to unseen data.

The Precision-Recall curves illustrate the trade-off between Precision and Recall across varying thresholds (Fig 2). The Precision-Recall (PR) curve presented demonstrates the model's performance for the "Canopy" class. With a mean Average Precision (mAP) of 0.975 at IoU 0.5, the graph indicates a high precision across a wide range of recall values, signifying the model's robustness in accurately identifying and segmenting plants.

The high mAP scores reflect the model's ability to balance false positives and false negatives effectively. The consistency across IoU thresholds highlights YOLOv11's capability to delineate canopy boundaries with precision.

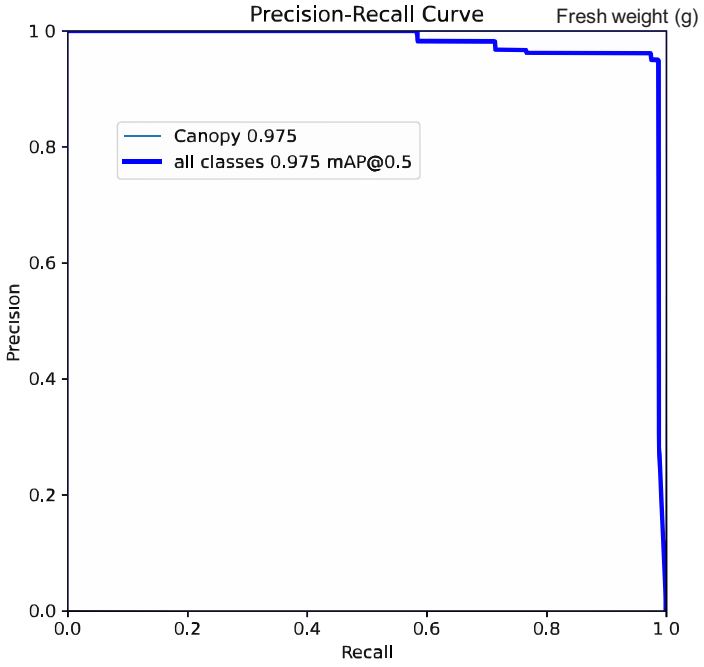

Fig 2. Precision-recall curve with mean average precision score

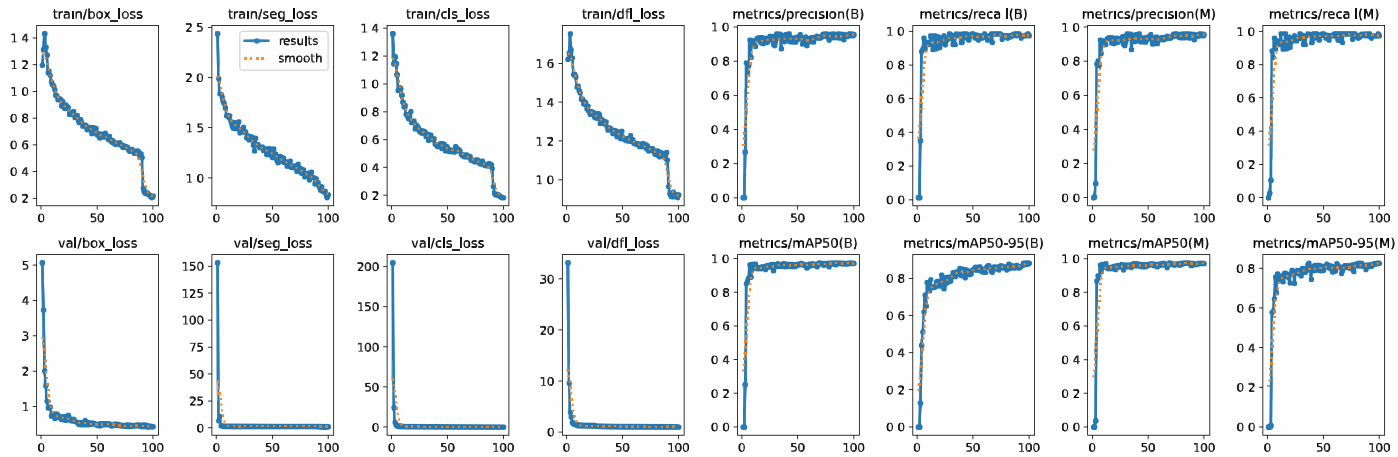

Fig 1. Training and validation loss curves for YOLOv11 with 100 epochs

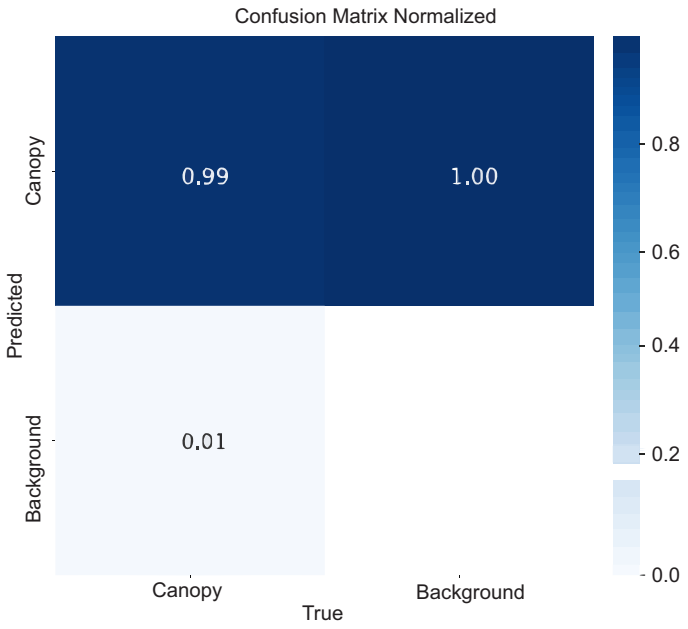

Fig. 3. Normalized confusion matrix of YOLO11 segmentation

The confusion matrix and normalized confusion matrix (Fig 3) provide an overview of classification accuracy for the canopy segmentation task. The majority of predictions fell within the true positive category, with minimal misclassification.

The normalized confusion matrix shows YOLOv11's performance in segmenting plant canopies. The matrix shows a high True Positive Rate (TPR) of 99% for the "Canopy" class and minimal misclassification (1% false negatives for the background class), indicating excellent model accuracy and reliability. The background is almost entirely correctly classified with a False Positive Rate (FPR) close to 0%. This highlights YOLOv11's robustness in distinguishing between canopy and non-canopy regions effectively.

The F1-Confidence curve demonstrates the model's performance across varying confidence thresholds, with the highest F1-Score of 0.97 achieved at a confidence level of 0.798 (Fig. 4). This

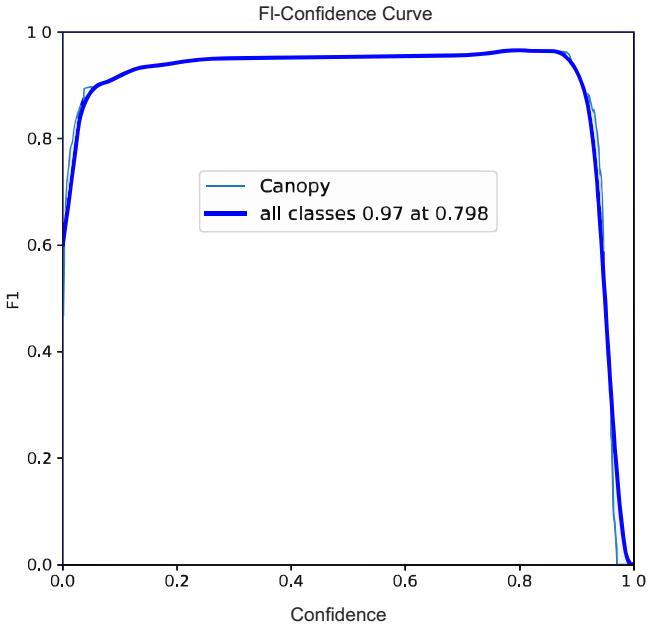

Fig 4. F1-Confidence curve for YOLOv11 segmentation

indicates an optimal balance between precision and recall, highlighting the model's robustness in accurately segmenting tomato plant canopies.

The sharp decline beyond the peak underscores the importance of selecting an appropriate confidence threshold to maintain accuracy. As the confidence threshold increases, the model becomes more selective, balancing precision and recall to achieve a higher F1-Score. In this case, the F1-Score rapidly peaks at 0.970 around a confidence threshold of 0.798, indicating the model's optimal performance.

The consistently high Intersection over Union (IoU) scores calculated at multiple thresholds underscore the model's robustness in accurately segmenting canopy regions, even in challenging scenarios with overlapping or densely packed structures. For instance, IoUs of 0.890 at a threshold of 0.5 and 0.84 at a threshold of 0.75 indicate the model's ability to maintain precision across different levels of overlap between predicted and ground-truth masks. These results validate YOLOv11's effectiveness in preserving boundary details and accurately delineating canopy regions.

Building upon these segmentation results, the study focused on leveraging the segmented canopy regions for feature analysis. The plant images captured from the field were accurately segmented and delineated the canopy regions (Fig. 5 b). The segmented images were further processed to binary format to enhance computational efficiency, with canopy pixels assigned a value of 1 and background pixels set to 0 (Fig 5c). This binary conversion facilitates subsequent feature extraction while preserving essential structural details.

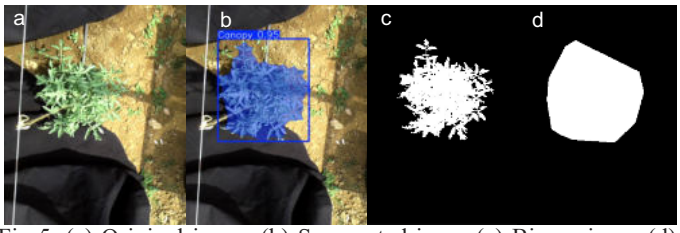

Fig 5. (a) Original image (b) Segmented image(c) Binary image(d) Convex hull area

The digital biomass was computed as the total count of pixels within the segmented canopy region, representing the plant's overall size. Additionally, the convex hull area, defined as the smallest convex polygon enclosing the canopy, was calculated to assess the spatial spread of the plant (Fig. 5d). The compactness, quantified as the ratio of digital biomass to the convex hull area, provided insights into canopy density and growth patterns.

The illustration in Fig. 6 shows the strong positive relationship between fresh biomass (g) and digital biomass (pixels) derived from YOLO11-segmented canopy images. Linear regression revealed a strong association between destructively measured fresh weight and image-derived digital biomass ($R^2 = 0.821$, $P < 0.001$), with an RMSE of 8,937 for the validation dataset (n = 100). A pooled linear regression across all observations confirmed the robustness of this relationship over a wide range of plant sizes. Model diagnostics indicated that regression assumptions were satisfied, with residuals exhibiting approximate normality (Shapiro–Wilk test, $P = 0.717$) and homoscedasticity (Breusch–Pagan test, $P = 0.485$). Influence diagnostics based on Cook's

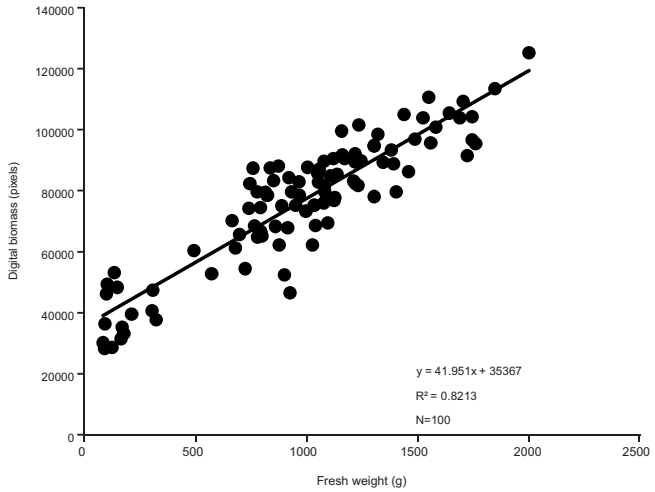

Fig. 6. Relationship between digital biomass and actual fresh weight for validation

distance indicated that no single observation disproportionately affected the regression fit. These results validate the reliability of YOLO11-derived digital biomass as a robust, non-invasive proxy for fresh biomass estimation, supporting its applicability for scalable crop monitoring in precision agriculture.

The digital biomass of four tomato genotypes with three replications was analyzed across two growth stages (flowering and fruiting) under 100% and 50% irrigation regimes, highlighting the influence of water availability and growth stage on biomass accumulation (Fig. 6). The analysis of digital biomass, convex hull area, and compactness allowed the identification of genotypes under two irrigation regimes and growth stages. Thus, highlighting (Table 2) the performance of four tomato genotypes (Arka Rakshak, Arka Abhed, Arka Vikas, and Arka Meghali) across two irrigation regimes (100% and 50%) and two growth stages (Flowering and Fruiting) using three image-derived parameters: digital biomass, convex hull area, and compactness.

Table 2 provides insights into the digital biomass of four tomato genotypes across two growth stages (Flowering and Fruiting) for 100% irrigation. Under 100% FC irrigation, Arka Rakshak demonstrated the highest digital biomass during the flowering stage, whereas Arka Abhed outperformed all other genotypes during the fruiting stage, achieving the highest digital biomass. ○

Table 2. Image-derived parameters of tomato genotypes across 100% of flowering and fruiting stages

Genotype	100% irrigation		
	Digital Biomass (pixels)	Convex Hull Area (pixels)	Compactness
	Flowering		
Arka Rakshak	58,814 ± 582^{e}	98,485 ± 308^{f}	0.597 ± 0.004^{b}
Arka Abhed	57,841 ± 931^{e}	93,421 ± 291^{g}	0.619 ± 0.008^{a}
Arka Vikas	49,110 ± 708^{f}	141,245 ± 701^{d}	0.348 ± 0.003^{e}
Arka Meghali	48,729 ± 510^{f}	76,971 ± 29^{h}	0.633 ± 0.006^{a}
	Fruiting		
Arka Rakshak	99,398 ± 481^{b}	179,880 ± 491^{b}	0.553 ± 0.002^{c}
Arka Abhed	108,919 ± 1,485^{a}	216,549 ± 2,607^{a}	0.503 ± 0.004^{d}
Arka Vikas	96,399 ± 272^{c}	164,138 ± 3,920^{c}	0.588 ± 0.014^{b}
Arka Meghali	72,140 ± 642^{d}	127,516 ± 1,458^{e}	0.566 ± 0.011^{c}

Values are means ± standard error (SE) from three biological replications (n = 3). Different superscript letters within each column indicate significant differences according to Duncan's Multiple Range Test (DMRT) at $P< 0.05$

In the 50% irrigation treatment (Table 3), Arka Vikas recorded the highest digital biomass at the flowering stage, indicating its relative tolerance to water stress during early growth, while Arka Abhed excelled during the fruiting stage with the highest digital biomass. These results highlight genotype-specific differences in biomass production, with Arka Rakshak and Arka Abhed performing better under optimal irrigation, and Arka Vikas and Arka Rakshak showing resilience under water-limited conditions.

Table 3. Image-derived parameters of tomato genotypes under 50% across the flowering and fruiting stages

Genotype	50% irrigation		
	Digital Biomass (pixels)	Convex Hull Area (pixels)	Compactness
	Flowering		
Arka Rakshak	38,912 ± 283^{f}	66,719 ± 260^{g}	0.583 ± 0.005^{c}
Arka Abhed	43,842 ± 495^{e}	83,421 ± 575^{f}	0.526 ± 0.002^{d}
Arka Vikas	44,888 ± 496^{e}	88,452 ± 796^{e}	0.507 ± 0.002^{e}
Arka Meghali	24,404 ± 301^{g}	39,971 ± 106^{h}	0.611 ± 0.009^{b}
	Fruiting		
Arka Rakshak	74,588 ± 248^{c}	113,158 ± 1,703^{d}	0.659 ± 0.009^{a}
Arka Abhed	83,643 ± 198^{a}	165,811 ± 789^{b}	0.504 ± 0.004^{e}
Arka Vikas	81,102 ± 23^{b}	139,131 ± 647^{c}	0.583 ± 0.003^{c}
Arka Meghali	60,141 ± 189^{d}	174,836 ± 1,791^{a}	0.344 ± 0.002^{f}

Values are means ± standard error (SE) from three biological replications (n = 3). Different superscript letters within each column indicate significant differences according to Duncan's Multiple Range Test (DMRT) at $P< 0.05$

The images explicitly demonstrate morphological differences in plant canopies across irrigation treatments (100% and 50% FC) and growth stages (flowering and fruiting) using image-derived parameters such as canopy density and convex hull area (Fig 7a and 7 b). The progression from original images to segmented, binary, and convex-hull representations highlights structural changes in canopy morphology.

The convex hull area, which outlines the smallest polygon enclosing the canopy, provides a spatial measure of the canopy's extent. This parameter is used to derive compactness, calculated as the ratio of digital biomass to the convex hull area, effectively quantifying canopy density. Under optimal irrigation (100%), the images reveal larger, well-spread canopies with higher convex hull areas, reflecting robust growth.

Under water stress (50% FC), reduced canopy size and fragmented structures are evident, particularly in the binary and convex hull images, indicating the morphological impact of water limitations. Compactness derived from these images helps to capture canopy density, allowing clear distinctions between dense and sparse canopies across treatments and growth stages, providing a non-invasive method to evaluate genotype performance.

Discussion

Digital biomass serves as a direct measure of plant growth, while the convex hull area captures the overall canopy size and spatial distribution. These metrics provide a robust foundation for distinguishing control plants from those subjected to stress,

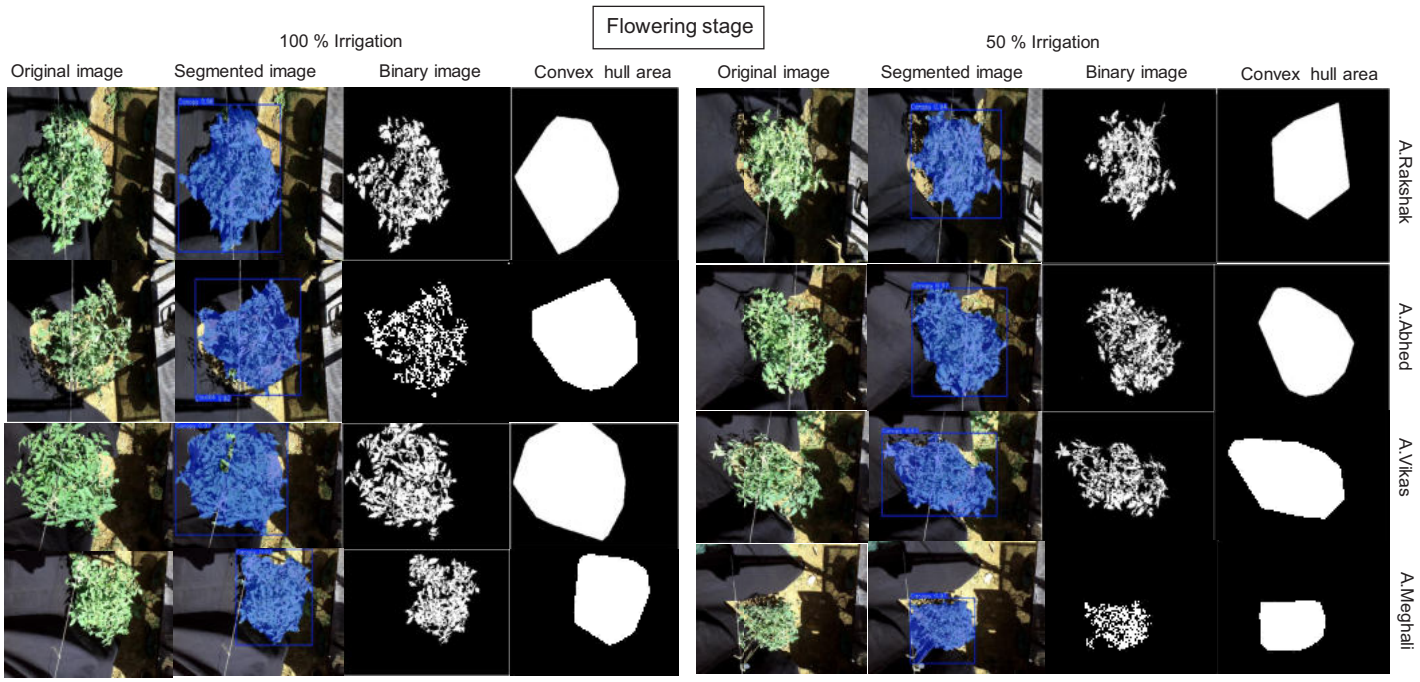

Fig. 7a . Visualization of canopy morphology across irrigation treatments at the flowering stage

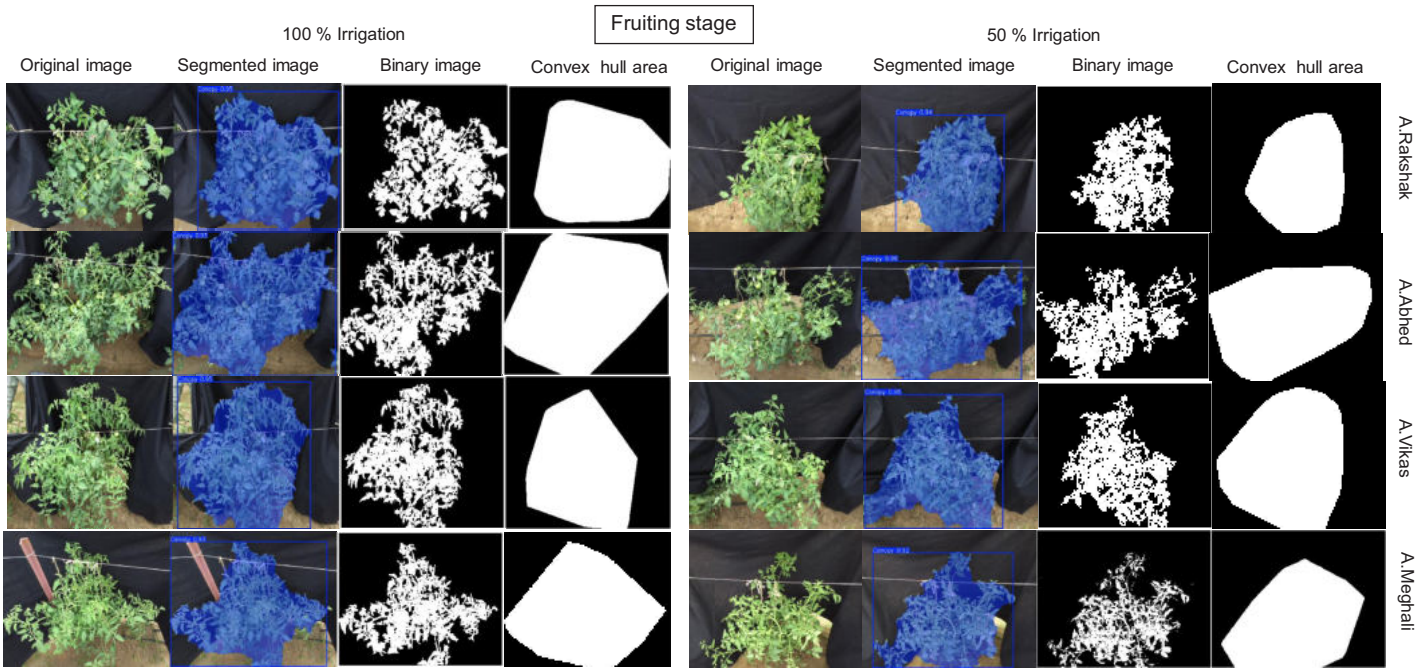

Fig. 7b. Visualization of canopy morphology across irrigation treatments at fruiting stage

as stress typically induces structural changes in the canopy, including reduced convex hull areas and altered canopy density (Zhou *et al.,* 2022).

In addition to these metrics, derived parameters, such as compactness, defined as the ratio of digital biomass to the convex hull area, further enhance the ability to assess canopy structure and stress levels (Zhou *et al.,* 2017). Compactness serves as an indicator of canopy density and cover, providing valuable insights into plant health and growth (Neilson *et al.,* 2015). Recent phenotyping advancements have operationalized compactness not merely as a function of leaf area, but as a distinct morphological descriptor of the canopy architecture. Zhou *et al*. (2025) utilized compactness to explicitly characterize the 'arrangement and density' of plant structures, while Wu *et al*. (2022) demonstrated its utility in differentiating shoot architecture across cultivars. Consistent with these approaches, our results indicate that digital compactness serves as a robust, standalone signature of stress-induced geometric contraction and a means to monitor structural responses to water deficit, without necessitating additional parameters.

Stress detection is an integral aspect of precision agriculture, as timely identification and quantification of stress can significantly improve crop management strategies and mitigate yield losses (Geckeler *et al.,* 2023). These stressors often lead to observable changes in canopy structure, such as reduced leaf area, altered canopy density, and diminished growth (Weng *et al.,*2023).

Advanced segmentation outputs from YOLO11 enable accurate quantification of these morphological changes, enabling precise and scalable stress detection.

While the foundational studies by Laxman *et al*. (2018, 2022) successfully utilized RGB imaging, their methodology relied on color-based thresholding using proprietary software. Such pixel-level approaches depend heavily on specific color intensities (e.g., greenness) to define the plant. In contrast, the present study employs YOLO11, which was trained using whole-canopy annotations rather than pixel-color thresholds. By learning from these canopy-level segmentations, the model identifies the plant as a unified structural entity based on learned morphological features. This approach is robust against spectral variability and enables the precise extraction. The combination of digital biomass and convex hull metrics provides a comprehensive framework for assessing the impacts of stress on plant canopies. For instance, the convex hull area captures the canopy's overall spatial footprint, while compactness quantifies the canopy's density relative to its spatial extent. This capability is particularly beneficial in horticultural crops, where early stress detection can guide irrigation, fertilization, and other management practices (Abebe *et al.,* 2023).

Beyond stress detection, this methodology extends its utility to high-throughput phenotyping to understand genotypic variability and identify traits associated with stress tolerance (Jangra *et al.,* 2021). This high-throughput approach facilitates the evaluation of genotypic differences under varying environmental conditions (Wu *et al.,* 2021), supporting breeding programs aimed at developing resilient crops (Danilevicz *et al.,* 2021). The ability to detect subtle variations in stress responses across multiple genotypes underscores the transformative potential of integrating advanced technologies with plant science (Choudhury *et al*., 2019). This comprehensive approach not only enables accurate assessment of stress-induced structural changes in plant canopies but also facilitates evaluation of genotypic variability, supporting breeding programs for resilient crop varieties and advancing precision agriculture toward sustainable, efficient crop management.

This study developed and validated a deep learning-based framework for non-invasive biomass estimation and stress-responsive canopy characterization in tomato plants using the YOLOv1 model. The proposed approach achieved high canopy segmentation performance (m*AP*= 0.975). It demonstrated a strong linear relationship between image-derived digital biomass and destructively measured fresh weight ($R^2 = 0.821$), confirming the reliability of RGB image–based phenotyping across growth stages and irrigation regimes. Digital canopy traits, including digital biomass and compactness, effectively captured genotype- and treatment-specific structural responses to water stress, highlighting their utility for stress differentiation and phenotypic assessment.

Compared with conventional destructive biomass and leaf area measurements, which are typically time-consuming and labor-intensive, the proposed image-based workflow enables trait extraction faster using low-cost RGB imaging. This represents a substantial gain in throughput and scalability, while allowing continuous monitoring of the same plants throughout the growing season. Such efficiency makes the approach particularly suitable for large-scale field deployment and real-time crop monitoring.

From an application perspective, the framework is readily adaptable to IoT-enabled agricultural systems. Canopy images acquired using field cameras, handheld devices, or mobile platforms can be processed on edge devices, with extracted phenotypic traits transmitted to cloud-based dashboards for real-time visualization and decision support. Overall, this study demonstrates the potential of YOLO11-based image phenotyping as a scalable and cost-effective component of precision horticulture, contributing to sustainable crop management.

Acknowledgment

This work was supported by the National Innovations in Climate Resilient Agriculture (NICRA) project of the Indian Council of Agricultural Research.

References

Abebe A.M., Y. Kim, J. Kim, S.L. Kim and J. Baek, 2023. Image-based high-throughput phenotyping in horticultural crops. *Plants*, 12(10): 2061. https://doi.org/10.3390/plants12102061

Danilevicz M.F., P.E. Bayer, B.J. Nestor, M. Bennamoun and D. Edwards, 2021. Resources for image-based high-throughput phenotyping in crops and data sharing challenges. *Plant Physiol.*, 187(2): 699-715. https://doi.org/10.1093/plphys/kiab301

Das Choudhury S., A. Samal and T. Awada, 2019. Leveraging image analysis for high-throughput plant phenotyping. *Front. Plant Sci.*, 10: 508. https://doi.org/10.3389/fpls.2019.00508

Decker S.R., A.E. Harman-Ware, R.M. Happs, E.J. Wolfrum, G.A. Tuskan, D. Kainer, G.B. Oguntimein, M. Rodriguez, D. Weighill, P. Jones and D. Jacobson, 2018. High-throughput screening technologies in biomass characterization. *Front. Energy Res.*, 6: 120. https://doi.org/10.3389/fenrg.2018.00120

Desai S.Y. and S.L. Kore, 2025. Object detection and segmentation in indian flat bread chapati using AI models. *Eng. Technol. Appl. Sci. Res.*, 15(5): 26163-26170. https://doi.org/10.48084/etasr.12088

Geckeler C., S.E. Ramos, M.C. Schuman and S. Mintchev, 2023. Robotic volatile sampling for early detection of plant stress: Precision agriculture beyond visual remote sensing. *IEEE Robot. Autom. Mag.* https://doi.org/10.1109/MRA.2023.3315932

Hagn L., J. Schuster, M. Mittermayer and K.J. Hülsbergen, 2024. A new method for satellite-based remote sensing analysis of plant-specific biomass yield patterns for precision farming applications. *Precis. Agric.*, pp: 1-30. https://doi.org/10.1007/s11119-024-10144-x

Jain S., D. Ramesh, E. Damodar Reddy, S. Rathod and G. Ondrasek, 2024. A fast high throughput plant phenotyping system using YOLO and Chan-Vese segmentation. *Soft Comput.*, 28(20): 12323-12336. https://doi.org/10.1007/s00500-024-09946-y

James, N., and M. Umesh, 2025**.** Improved tomato (*Solanum lycopersicum* L.) growth and reduction of fungal pathogens utilising the plant growth-promoting and antifungal *Bacillus albus* NJ01 as a bioinoculant. *J. Appl. Hortic.*, **27**(2): 215–220.

Jangra S., V. Chaudhary, R.C. Yadav and N.R. Yadav, 2021. High-throughput phenotyping: A platform to accelerate crop improvement. *Phenomics*, 1(2): 31-53. Johansen K., M.J. Morton, Y. Malbeteau, B. Aragon, S. Al-Mashharawi, M.G. Ziliani, Y. Angel, G. Fiene, S. Negrão, M.A. Mousa and M.A. Tester, 2020. Predicting biomass and yield in a tomato phenotyping experiment using UAV imagery and random forest. *Front. Artif. Intell.*, 3: 28. https://doi.org/10.3389/frai.2020.00028

Khanam R. and M. Hussain, 2024. YOLOv11: An overview of the key architectural enhancements. *arXiv preprint arXiv:2410.17725*.

Laxman R.H., P. Hemamalini, M.R. Namratha, R.M. Bhatt and A.T. Sadashiva, 2022. Phenotyping deficit moisture stress tolerance in tomato using image-derived digital features. *Int. J. Bio-resour. Stress Manag.*, 13(4): 339-347. https://doi.org/10.23910/1.2022.2544

Laxman R.H., P. Hemamalini, R.M. Bhatt and A.T. Sadashiva, 2018. Non-invasive quantification of tomato (Solanum lycopersicum L.) plant biomass through digital imaging using phenomics platform. *Indian J. Plant Physiol.*, 23: 369-375. https://doi.org/10.1007/s40502-018-0374-8

Li Z., R. Guo, M. Li, Y. Chen and G. Li, 2020. A review of computer vision technologies for plant phenotyping. *Comput. Electron. Agric.*, 176: 105672. https://doi.org/10.1016/j.compag.2020.105672

Mahdy, H.A., A.S. Tantawy, A.M.R. Abdel-Mawgoud and Z.F. Fawzy, 2024. Physiological and growth attributes of salt-stressed tomato plants in response to foliar application of nano phosphorus or potassium. *J. Appl. Hortic.*, 26(1): 68–72.

Neilson E.H., A.M. Edwards, C.K. Blomstedt, B. Berger, B.L. Møller and R.M. Gleadow, 2015. Utilization of a high-throughput shoot imaging system to examine the dynamic phenotypic responses of a C4 cereal crop plant to nitrogen and water deficiency over time. *J. Exp. Bot.*, 66(7): 1817-1832. https://doi.org/10.1093/jxb/eru526

Paul A., R. Machavaram, D. Kumar and H. Nagar, 2024. Smart solutions for capsicum harvesting: Unleashing the power of YOLO for detection, segmentation, growth stage classification, counting, and real-time mobile identification. *Comput. Electron. Agric.*, 219: 108832. https://doi.org/10.1016/j.compag.2024.108832

Rahman, M.M., M.S. Rahman, M.G.J. Helal, M.Z.K. Roni and J. Uddain, 2025. Potential impacts of gibberellic acid to promote salinity tolerance in tomato. *J. Appl. Hortic.*, 27(1): 51–56.

Redmon J., 2016. You only look once: Unified, real-time object detection. In: *Proc. IEEE Conf. Comput. Vis. Pattern Recognit.* https://doi.org/10.1109/CVPR.2016.91

Ritchie H., P. Rosado and M. Roser, 2023. Agricultural production. *Our World in Data*. https://ourworldindata.org/agricultural-production

Rocha Júnior D.S., A.C. Barbosa, I.A. Batista, L.R. Camillo, N.S. Lopes and M.G. Costa, 2023. Impact of moderate water deficit at the fruit development stage of tomato (*Solanum lycopersicum* L.): Effects on plant growth, physiology, fruit yield and quality and expression of carotenoid biosynthesis genes. *Acta Physiol. Plant.*, 45(5): 65. https://doi.org/10.1007/s11738-023-03549-0

Smith D.T., A.B. Potgieter and S.C. Chapman, 2021. Scaling up high-throughput phenotyping for abiotic stress selection in the field. *Theor. Appl. Genet.*, 134(6): 1845-1866. https://doi.org/10.1007/s00122-021-03864-5

Tripodi P., C. Vincenzo, A. Venezia, A. Cocozza and C. Pane, 2024. Precision phenotyping of wild rocket (*Diplotaxis tenuifolia*) to determine morpho-physiological responses under increasing drought stress levels using the PlantEye multispectral 3D system. *Horticulturae*, 10(5): 496. https://doi.org/10.3390/horticulturae10050496

Weng S., J. Ma, W. Tao, Y. Tan, M. Pan, Z. Zhang, L. Huang, L. Zheng and J. Zhao, 2023. Drought stress identification of tomato plant using multi-features of hyperspectral imaging and subsample fusion. *Front. Plant Sci.*, 14: 1073530. https://doi.org/10.3389/fpls.2023.1073530

Wu S., W. Wen, W. Gou, X. Lu, W. Zhang, C. Zheng, Z. Xiang, L. Chen and X. Guo, 2022. A miniaturized phenotyping platform for individual plants using multi-view stereo 3D reconstruction. *Front. Plant Sci.*, 13: 897746. https://doi.org/10.3389/fpls.2022.897746

Wu X., F. Zheng, G. Xu, K. Yang, D.R. Clements, Y. Yang, S. Yang, G. Jin, F. Zhang and S. Shen, 2024. Plant growth and physiological responses of the invasive plant Acmella radicans to contrasting light and soil water conditions. *Discover Life*, 54(1): 11. https://doi.org/10.1007/s11084-024-09656-3

Wu X., H. Feng, D. Wu, S. Yan, P. Zhang, W. Wang, J. Zhang, J. Ye, G. Dai, G. Fan and W. Li, 2021. Using high-throughput multiple optical phenotyping to decipher the genetic architecture of maize drought tolerance. *Genome Biol.*, 22: 1-26. https://doi.org/10.1186/s13059-021-02377-0

Zhou J., C. Applegate, A.D. Alonso, D. Reynolds, S. Orford, M. Mackiewicz, S. Griffiths, S. Penfield and N. Pullen, 2017. Leaf-GP: An open and automated software application for measuring growth phenotypes for Arabidopsis and wheat. *Plant Methods*, 13: 1-7. https://doi.org/10.1186/s13007-017-0266-3

Zhou L., X. Li, B. Zhang, J. Xuan, Y. Gong, C. Tan, H. Huang and H. Du, 2022. Estimating 3D green volume and aboveground biomass of urban forest trees by UAV-lidar. *Remote Sens.*, 14(20): 5211. https://doi.org/10.3390/rs14205211

Zhou L., Z. Tang, S. Cao, X. Hu, W. Zhou, X. Zhu, X. Bai, H. Lu, F. Chen and W. Hu, 2025. TillerPET: high-throughput in-situ phenotyping of rice tiller number and compactness from post-harvest stubble. *Crop J.* https://doi.org/10.1016/j.cj.2025.09.022

Received: November, 2025; Revised: November, 2025;
Accepted: December, 2025